Arthropod Structure & Development 45 (2016) 509–518

Contents lists available at ScienceDirect

Arthropod Structure & Development

journal homepage: www.elsevier.com/locate/asd

Structural and physical evidence for an endocuticular gold reflector in the tortoise beetle, *Charidotella ambita*

Jacques M. Pasteels [a], Olivier Deparis [b], Sébastien R. Mouchet [b, c], Donald M. Windsor [d], Johan Billen [e, *]

[a] Université Libre de Bruxelles, Evolutionary Biology and Ecology, C.P. 160/12, Avenue F.D. Roosevelt 50, B-1050 Brussels, Belgium
[b] University of Namur (UNamur), Department of Physics, Physics of Matter and Radiation (PMR), Rue de Bruxelles 61, B-5000 Namur, Belgium
[c] University of Exeter, College of Engineering, Mathematics and Physical Sciences, Stocker Road, Exeter EX4 4QL, United Kingdom
[d] Smithsonian Tropical Research Institute, Apartado 0843-03092, Balboa, Ancon, Panama City, Panama
[e] KU Leuven, Zoological Institute, Naamsestraat 59, Box 2466, B-3000 Leuven, Belgium

ARTICLE INFO

Article history:
Received 4 July 2016
Received in revised form
3 October 2016
Accepted 5 October 2016
Available online 22 October 2016

Keywords:
Elytra
Ultrastructure
Structural color
Gold reflector
Tortoise beetle
Chrysomelidae

ABSTRACT

Charidotella ambita offers a unique opportunity for unambiguously locating its gold reflector by comparing the structure of reflecting and non-reflecting cuticle of the elytron and pronotum. Using light microscopy and TEM, the reflector was located underneath the macrofiber endocuticle just above the epidermis. The reflector is a multilayer comprising up to 50 bilayers alternating high and low density layers parallel to the surface of the cuticle. It is chirped, i.e., showing a progressive decrease in layer thickness from approximately 150 nm–100 nm across its depth. The high density layers in contact with the endocuticle fuse to the last macrofiber when the reflector is interrupted by a trabecula, demonstrating their cuticular nature. Simulated reflectance spectra from models of the multilayer matched the reflection spectra measured on the major gold patch of the elytron of living specimens.

Previous reports in adult insects exhibiting metallic colors located their reflector in the upper strata and structures of the cuticle, i.e., epicuticle, exocuticle, scales and hairs. Thus, the endocuticular location of the reflector in *C. ambita* (and other tortoise beetles) appears unique for adult insects. Gold reflection appears in *C. ambita* only when the synthesis of the macrolayer endocuticle is complete, which may take up to 2 weeks. The development of the gold reflector coincides with the start of mating behavior, possibly suggesting a signaling function in conspecific recognition once sexual maturity has been reached.

1. Introduction

The family name chosen by Linnaeus for leaf beetles, Chrysomelidae, was derived from the Greek for “gold beetles” (Greek χρυσομηλον, literally ‘golden apple’, influenced by χρυσομηλολόνθιον ‘little golden chafer’). No doubt Linnaeus who first coined the type genus name *Chrysomela* from which Chrysomelidae was later derived, was responding to the brilliant “metallic” colors of the beetles he included in this taxon (presently including both genera, *Chrysomela* and *Chrysolina*). Metallic colors are not just the privilege of leaf beetles, but occur widely throughout the Arthropoda, e.g., jumping spiders. The coloration in most of these derives from the multilayered structure of the hard, dry, peripheral layer of the exoskeleton (e.g., Neville and Caveney, 1969; Vigneron et al., 2006; Seago et al., 2009; Stavenga et al., 2011; Ingram et al., 2011), although an endocuticular reflector was reported in danaine pupae (Steinbrecht, 1985; Steinbrecht et al., 1985). Reflective metallic colors (or structural colors) produced by light interference are widespread in biology and are the subject of the active field of biophotonics, the search for bio-inspired materials (e.g., McPhedran and Parker, 2015). The layered exoskeleton of insects has presented natural selection many options for building structural colors, ranging from simple diffraction gratings to two- and three-dimensional photonic crystals in the scales of butterflies and beetles (Berthier, 2007). Metallic colors in Coleoptera are rarely pure gold, but instead are shiny, often iridescent, shades of yellow, green, blue and red. Pure gold reflectors are rarer, occurring in the

* Corresponding author.
E-mail addresses: jmpastee@ulb.ac.be (J.M. Pasteels), olivier.deparis@unamur.be (O. Deparis), sebastien.mouchet@unamur.be (S.R. Mouchet), windsordm@gmail.com (D.M. Windsor), johan.billen@kuleuven.be (J. Billen).

http://dx.doi.org/10.1016/j.asd.2016.10.008
1467-8039/

elytra and pronota of scarab beetles in the genus *Chrysina* and in the discal elytra and pronota of Cassidini and Aspidimorphini tortoise beetles (where lateral and frontal margins are usually transparent). Metallic colors may be permanent as in scarab beetles and tortoise beetles in the tribe Omocerini or they may be transient, degrading rapidly from the live state and totally absent in dead specimens. Permanently metallic-colored species are often sought after by amateur "collectors" in commercial insect fairs. The transient metallic coloration of tortoise beetles in the tribes Cassidini and Aspidomorphini vanishes in dead and dried specimens, and are replaced by a dull yellow or reddish brown color. To a limited extent, the reflective gold color can be restored when dried specimens are rehydrated (Mason, 1929).

Yet other tortoise beetles have the ability to reversibly shut down their reflectivity upon disturbance, switching quickly from bright gold to reddish brown or vivid red if a sub-epidermal red pigment layer is present. Later and less quickly the same beetles, when alive, can restore their gold coloration (Mason, 1929; Hinton, 1973; Jolivet, 1994; Vigneron et al., 2007b). This unique capacity was investigated in two species, the South African *Aspidomorpha tecta* (Hinton, 1973; Neville, 1977; Parker et al., 1998) and the Panamanian *Charidotella egregia* (Vigneron et al., 2007b). In both species, a chirped multilayer reflector was described in the cuticle, and the switch of color attributed to the amount of liquid secreted (or resorbed) by the epidermal cells between the cuticular lamellae, although the precise mechanism remained to be disclosed. As in dead specimens, the reflector would be shut down, and dehydrated. In *Aspidomorpha tecta*, the chirped reflector was located in the endocuticle, just above the epidermis as illustrated by a single TEM micrograph, obviously from a freshly fixed elytron, published by Hinton (1973), and further used by Neville (1977) and Parker et al. (1998) in their later analyses. In *C. egregia*, however, the chirped reflector was located in the exocuticle as were the reflectors of other colored beetles exhibiting metallic colors. SEM and TEM micrographs obtained from dead, dry elytra were published in support of this location by Vigneron et al. (2007b).

Metallic coloration in some Cassidini species is limited to specific regions of the elytra and pronotum, alternating with reddish brown or black regions to form specific elytral designs. This configuration is present in *Charidotella ambita*, a species with a "fixed reflector", unable to change color when alive, but lacking the gold color entirely in dead, dry specimens, where it is replaced by dull yellow or brown colors.

C. ambita offers a unique opportunity for comparing the ultrastructure of reflecting and non-reflecting cuticle unambiguously identified within elytra from a single individual. Gold reflection is initially absent in immature adult individuals developing slowly over several days and in this way offering a way to observe ontogenetic changes in the ultrastructure of reflecting and non-reflecting cuticle. In this paper, we describe cuticle structure for elytra and pronotum of mature and immature adults of *C. ambita*. We deduce a putative reflector based on this morphological analysis. We simulate reflectance from the modeled reflector with this structure, which is then compared to that measured on living and freshly killed beetles.

2. Material and methods

Ten mature and two immature adults (age unknown) were collected on May 5, 2015, in El Copé (8.670°N, 80.593°W; Coclé Province, República of Panamá) while feeding on their host plant, *Ipomoea* sp. aff. *trifida* (Convolvulaceae). The immature adults were distinguished from mature adults by the lack of gold reflection and a softer cuticle. Five mature and two immature beetles from this collection were later fixed for TEM observations. Five mature beetles were kept alive for further spectroscopic measurements (in Namur, Belgium). Duplicate specimens were deposited as vouchers in the STRI reference insect collection and in the Museo de Invertebrados, Universidad de Panamá (MIUP).

Elytra were detached using microsurgery scissors and were cut transversely into anterior, median and posterior sections. The pronotal sclerite was cut longitudinally into two roughly equal pieces. The elytra and pronotal pieces were fixed overnight in cold 2% glutaraldehyde in a 50 mM Na-cacodylate buffer at pH 7.3 containing 150 mM saccharose. The pieces were rinsed in the buffer and kept in cold buffer until further processing.

After postfixation in 2% osmium tetroxide in the same buffer and dehydration in a graded acetone series, tissues were embedded in Araldite. Semi-thin sections with a thickness of 1 μm were made with a Leica EM UC6 ultramicrotome, stained with methylene blue and thionin before examination under an Olympus BX-51 microscope. Thin sections of 70 nm thickness were double stained with lead citrate and uranyl acetate, and examined under a Zeiss EM900 electron microscope. Material for scanning microscopy was mounted on a stub, coated with gold and examined in a JEOL JSM-6360 scanning microscope.

Reflection spectra ($R = I - B/W - B$) were measured using an Avantes AvaSpec-2048-2 fiber optic spectrophotometer and an Avantes AvaLight-DH-S-BAL deuterium/halogen light source. The measured spectra I were normalized with respect to the intensity W reflected by a white reference standard Avantes WS-2, with correction B for experimental optical and electronic noises and with respect to their respective maxima. The measurements were performed with a bifurcated optical fiber normal to the sample (guiding incident light to the sample and reflected light to the spectrophotometer). Live beetles were cooled during 20 min at 4 °C before measurement and positioned so that spectra were measured on the flatter section of the elytra.

The ultrastructure of the gold reflector was modeled as a planar multilayer stack. In different regions of the endocuticle (semi-ovoid central patch, explanate margin border), the multilayer stack could be recognized on the TEM micrographs from a typical pattern of alternating bright and dark layers. Along a line perpendicular to the stack, layers were counted and their thicknesses measured with the help of image processing software (ImageJ, Schneider et al., 2012). Thickness sampling error was estimated to 10%. Since the cuticle material consists of chitin microfibers in a protein matrix, density variations of chitin within the matrix modify the layer appearance (grey level) in TEM observations, i.e. dark layers are more dense than bright ones. Based on the reported refractive index value of pure chitin ($n_c = 1.56$ [Sollas, 1907; Leertouwer et al., 2011]), refractive indices of bright and dark layers were assumed to be around $n_b = 1.40$ and $n_d = 1.60$, respectively (combinations of slightly different values were tested in order to check the sensitivity of simulations to these parameters). From these refractive index values and layer thickness data, the reflectance spectrum of the multilayer stack was calculated at normal incidence using a computer code which implements the exact solutions of Maxwell's equations in arbitrarily stratified media (Vigneron and Lousse, 2006). The refractive indices of incidence and emergence semi-infinite media surrounding the multilayer stack were taken equal to $n_i = 1.0$ (air) and n_d (more dense cuticle), respectively.

From both experimentally normalized reflection and numerical reflectance spectra, chromaticity coordinates (x; y) were calculated (assuming a standard illuminant D65) following a method presented elsewhere (Judd and Wyszecki, 1975; Chamberlin and Chamberlin, 1980) and represented in the CIE 1931 color space chromaticity diagram.

3. Results

3.1. Color pattern and elytral structure

The discal area of the elytra and pronotum in tortoise beetles entirely covers the body and head and displays the color pattern characteristic of the species. In *C. ambita*, as in most species in the tribe Cassidini, only the discal area is colored. The explanate area marginal to the disc is near-perfectly transparent with a yellowish tinge arising from the cuticle material UV absorption band, the tail of which extends to the blue region of the visible spectrum. A delicate polygonal network of thin veins is visible in the same marginal area (Fig. 1A).

The elytral disc in *C. ambita* is black with a large semi-ovoid central gold patch, which reaches the sutural margin of each elytron. The central patches of each elytron form a larger ovoid area, divided longitudinally by a narrow medial band of black cuticle. A gold stripe encircles the disc where it meets the transparent margin (Fig. 1A). These gold areas are non-iridescent and appear metallic, i.e., their reflectance is high, broadband and restricted to the specular direction as in a metallic mirror. These properties are a first clue suggesting the presence of a chirped reflector, i.e., a multilayer stack of which the layer thicknesses vary across depth.

At rest, the elytra tightly attach to the body by a locking device located and concealed on the ventral face of the elytra. The anterior half of the elytron bears a small transverse (0.5 mm) flange or brace (Crowson, 1981; page 44) accompanied by a slightly longer (3 mm) longitudinal carina of approximately 0.5 mm parallel to the much higher and longer ridge separating the disc and the explanate margin (Fig. 1B and C). The anterior side of the abdomen is wedged between the ridges when elytra are locked.

The dorsal surface between the ridges is gold as it forms a part of the lateral gold ring. The longitudinal ridge and carina appear as "hooks" in cross sections (Fig. 1D) and locate the putative reflector in semithin and ultrathin sections (see below).

3.2. Light microscopy

A cross section of the right elytron is shown in Fig. 1D. Even at low magnification, the thin layer of black pigment in or on the epicuticle of the dorsal cuticle of the disc allows delimiting the black and gold regions proceeding from the sutural margin, left to the discal edge, where the transparent explanate margin starts. The hemolymph space in both black and gold regions is interrupted in places by cuticular bridges ('trabeculae' in Imms, 1934), where the dorsal and ventral cuticles fuse (Fig. 1E,G). Externally, the positions of trabeculae are indicated by small depressions forming distinct rows useful in taxonomic diagnoses. The punctate rows cross both color regions, which are not separated by a continuous cuticular barrier (Fig. 1F). Dorsal and ventral cuticle in the marginal area of the elytra is largely fused and lacking punctations with the hemolymph space reduced to a polygonal network of thin veins (Fig. 1D,H).

Gold reflecting regions possess a thickened layer at the basis of the dorsal cuticle and immediately above the epidermis (Fig. 1D–F). This layer is absent in the black regions (Fig. 1D,F,G), and in the veins of the explanate margin (Fig. 1D,H). In semithin sections, this layer appears homogenous, but ultimately proved to be a multilayer suggesting a putative reflector (see 3.3. Electron microscopy).

Fig. 1I is a longitudinal section of the pronotum where the transparent marginal area and the gold and black regions of the pronotal disc align as their equivalents do in the elytra. The anterior pronotal margin has a fused cuticle and network of thin veins without any thick layer between the epidermis and the cuticle. The gold region with epidermis and the putative reflector start at the discal ridge and are followed by black cuticle with pigment in or on the epicuticle but without the putative reflector at its base.

3.3. Ultrastructure of the dorsal cuticle of the elytra and pronotum

Cross sections of the elytron at the levels of the discal semi-ovoid gold patch and of the black discal region are shown in Fig. 2A and B. The only striking difference between the cuticles in both color regions is the occurrence of a thick multilayer between the epidermis and the last macrofiber of the endocuticle in the gold region. This multilayer was observed in the semi-thin sections only as a thick layer at optical microscope resolution without showing its true multilayer structure (Fig. 1). Exo- and endocuticles are similar in both color regions of the elytron and pronotum, and in the transparent marginal plates. Hence, they cannot be responsible for gold reflection and will only be briefly described.

The exocuticle is finely lamellate for a depth of 3.5 μm (Fig. 2C–E). The lamellae run parallel to the surface becoming progressively thicker with depth. The exocuticle is penetrated by a few thin pore canals at the top of the pore-canal network of the endocuticle (see below) which do not reach the surface of the cuticle. In the black region, the black pigment covers the exocuticle (Fig. 2D). Below the finely lamellate exocuticle, 3–4 layers, each about 320 nm in thickness, alternate with more electron dense layers, each about 200 nm in thickness, forming a transition zone between the exocuticle and the macrofibered endocuticle. Chitin microfibrils follow a twisted course, parallel to the surface.

The endocuticle is 25–30 μm thick and forms the bulk of the cuticle. In the black region (Fig. 2B), 14 macrofibers are present, each containing bundles of chitin microfibrils oriented differently in successive layers. The macrofibers progressively increase in thickness towards the center of the endocuticle reaching a maximum of 5 μm in thickness and then decrease in thickness toward the epidermis. The last macrofibers showing a successive change in orientation of microfibril bundles are about 0.5–0.3 μm in thickness. Two thin layers (0.2 μm), fused in place, follow above the epidermis and at this resolution appear to be lacking micro-fibrils.

There is a complex network of pore canals which follow irregular paths between the macrofibers and decrease gradually in width towards the exocuticle where they progressively disappear (see above). Depending on the orientation of the macrofibers in the micrographs, canals appear in sections as blades oriented parallel to the microfibril bundles, which further subdivide becoming increasingly narrow. The pore canals contain electron dense fibers appearing as dots in cross section (Fig. 3A, arrow). This canal network is formed by extensions of the epidermal cells between the macrofibers during their secretion (e.g., Leopold et al., 1992), as observed in micrographs of the cuticle of immature adults still in the progress of endocuticle synthesis (Fig. 3B). This structure of the endocuticle is similar in the black region of the pronotal disc and the marginal plates. Only slight variations in the number of fibers could be observed in some micrographs. It is also similar in all gold regions, but only ten distinct macrofibers were observed followed by a single layer of about 0.5 μm in which microfibrils are not distinguishable. Situated underneath is a multilayer up to 9.5 μm thick, showing all the structural features of a gold reflector (Figs. 2A, 4A).

Our description of the *C. ambita* multilayer is based on five micrographs obtained from gold regions chosen as objects for simulated reflectance spectra (see below): three from the semi-ovoid gold patch of the elytral disc (MLSO1, MLSO2, and MLSO3), and two from the gold lateral ring, of which one is within the elytron (MLER), and the other within the pronotum (MLPNR). The structure of the multilayer was similar in each of the five regions,

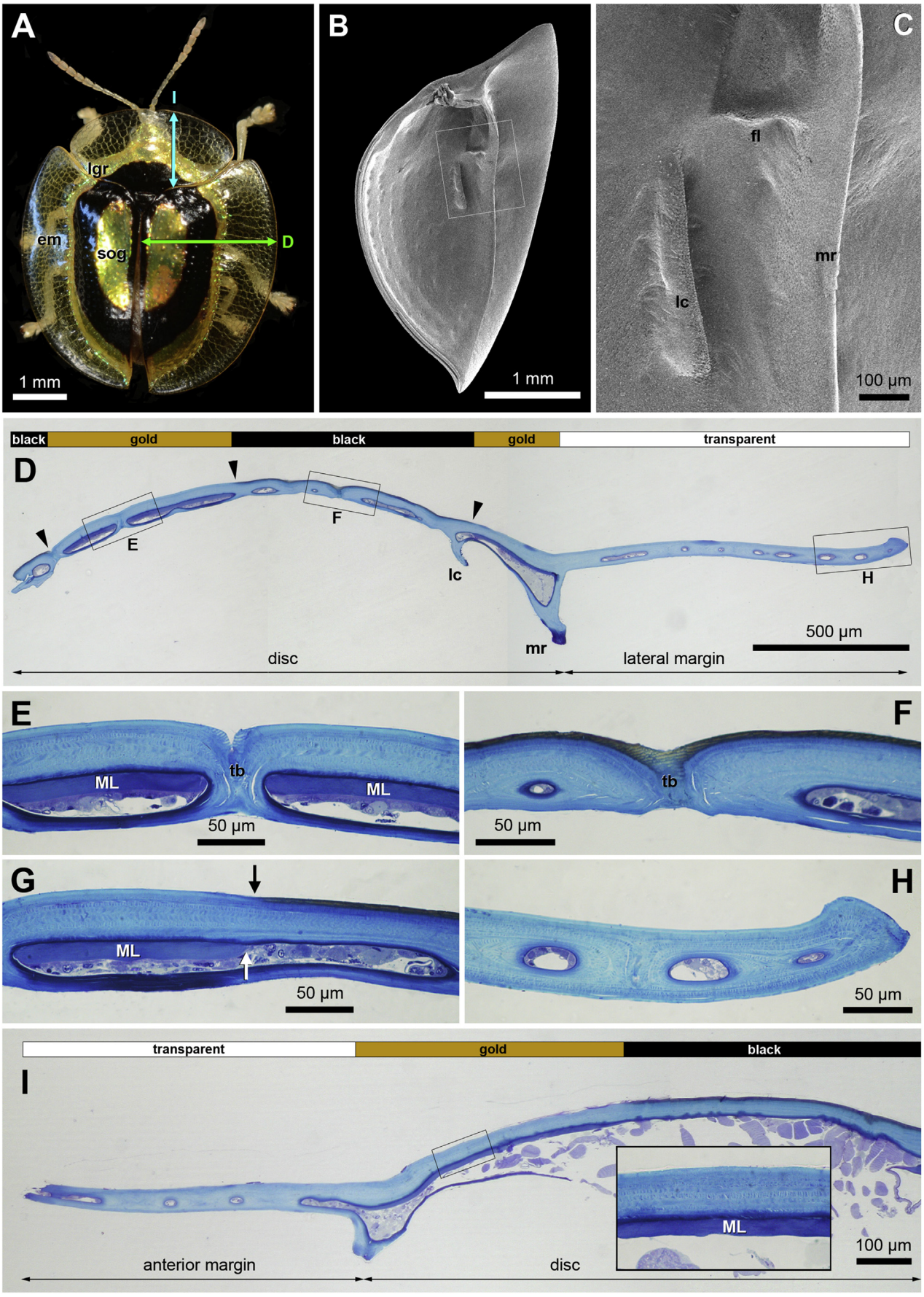
A
I
lgr
em
sog
D
1 mm
B
1 mm
C
fl
mr
lc
100 µm
black
gold
black
gold
transparent
D
E
F
lc
H
mr
500 µm
disc
lateral margin
E
ML
tb
ML
50 µm
F
tb
50 µm
G
ML
50 µm
H
50 µm
transparent
gold
black
I
ML
100 µm
anterior margin
disc

composed of successive bilayers parallel to the surface of the elytron with alternating weaker and stronger electron densities. The bilayers are highly regularly organized, as is needed for specular reflection. Multilayers MLSO1 and MLSO2 (Figs. 4A, 5) contained 53 bilayers whereas MLPNR had 52 bilayers. Smaller numbers of bilayers, 35 and 38, were found in MLER and in MLSO3 respectively, where layers fuse to the endocuticle of a trabecula or a cuticular ridge (Fig. 4B). Partial fusion of the first dark layers with the last 0.5 μm layer of the multilayered endocuticle is observed in Fig. 4A,C. The multilayers are noticeably "chirped", i.e. decrease progressively in layer thickness with depth which should generate a broad spectrum of reflected wavelengths (Fig. 4A–D). Bilayer thickness was measured along a line orthogonal to the layers, and is illustrated for MLSO2 in Fig. 5. The decrease in thickness was not linear, appearing exponential and stronger in the first 30 layers. This finding holds for both layer types, but less regularly for pale layers, which are more variable in thickness. These trends in layer thickness were observed in all multilayers examined (see Table S1, supplementary information). Both layer types contained microfibrils most likely composed of chitin without a distinct orientation. In the darker, less-electron dense layers, the microfibrils are connected to the surface of the electron dense layers in which the core is less dense than the surface (Fig. 4C). Narrow interruptions of the dense layers interconnect the light layers (Fig. 4D, arrow).

Multilayers were absent in the two young (teneral) adults examined lacking gold reflection. The epidermis in each was still secreting the macrofibers of the endocuticle (Fig. 3B).

3.4. Experimental reflection and simulated reflectance of gold areas

Normalized reflection spectra were measured at normal incidence on semi-ovoid gold patches of four different mature beetles (curves labeled #1–#4) and different areas of one mature specimen (curves labeled #4 (1–3)) (Fig. 6A and B). All spectra displayed low reflection at wavelengths shorter than 500 nm and a much higher reflection where they plateau at longer wavelengths. Distinct reflection bands (around 590, 690, 710 and 780 nm) were superimposed on this plateau in some cases. Depending on the area analyzed, the same specimen might or might not display such bands (Fig. 6A, curves labeled #4 (1–3)). These bands were typical of an "ordered" type of chirped reflector in which batches of layers of similar thickness are responsible for Bragg-like reflection peaks at specific depths, the coexistence of several such batches giving rise to broadband reflection. The chromaticity coordinates of each measured area were all located in the yellow region of the CIE diagram (Fig. 6B). Yellow hue and high specular reflection gave rise to the visual aspect of gold.

Simulated reflectance spectra confirmed the high, broadband reflection above 500 nm and the resulting yellowish color in a CIE diagram (Fig. 6C and D). Spectra were computed using layer thickness data collected from three different locations in the semi-ovoid central gold patch (MLSO1-3) and from the border gold ring of the elytra (MLER). Similar results, not shown, were found for the pronotum gold area. The typical shape of the simulated reflectance spectra is expected to be robust against the choice of refractive index which are difficult to estimate for cuticle material made of chitin fibers in a protein matrix. To verify this we tested combined index variations as large as $\Delta n_d = \pm 0.2$ and $\Delta n_b = \pm 0.2$ (i.e. absolute refractive index contrast variation as high as 0.4). As long as index contrast did not fall below n_d-$n_b = 0.2$, a high broadband reflection above 500 nm (see Fig. S1, supplementary information) was obtained.

4. Discussion

The structure of the dorsal exocuticle and macrofiber endocuticle is homogenous in all regions of the elytra and pronotum of *C. ambita* and conforms to that reported for other beetles, including other leaf beetles (e.g., Leopold et al., 1992; van de Kamp et al., 2016, and references therein). A transition zone between the finely lamellate exocuticle and the endocuticle was observed in the curculionid *Anthonomus grandis* (Leopold et al., 1992). The endocuticle composed of macrofiber layers, with bundles of microfibrils changing direction in successive layers, is observed commonly in insects, particularly in beetles (macrofiber cuticles of van de Kamp et al., 2016). The network of canals containing pore-canal fibers, following a serpentine, zig-zag, route through the endocuticle and ending in the exocuticle, is similar to that described in *A. grandis* (Leopold et al., 1992). In the black regions, the pigment, most likely melanin, is located in or above the epicuticle. A more detailed description of the ultrastructure of the *C. ambita* cuticle is beyond the scope of the present study.

The only structure in the cuticle that can be acting as a gold reflector is the endocuticular multilayer situated just above the epidermis and present in all gold regions of the elytra and pronotum but nowhere else. The endocuticular multilayer is not yet formed in young adults lacking gold reflectance in which the endocuticular macrofibers are still in formation. However, the pigment in the epicuticle of the black regions is already present at emergence and in older teneral adults. The regular and chirped structure of the endocuticular multilayer produces in mature adults a specular broadband reflection in wavelengths above 500 nm which gives rise to yellow color. Reflectance simulations based on four different multilayer micrographs from the elytron are in good agreement with the experimental reflection spectra obtained from the semi-ovoid gold region of the elytron.

Measured reflection spectra display high reflection at wavelengths longer than 500 nm. In some cases, distinct reflection bands (around 590, 690, 710 and 780 nm) are observed. Actually, this pattern comprising a plateau where distinct reflection bands are superimposed was already observed for the gold elytra of *C. egregia* (Vigneron et al., 2007b). The presence (or absence) of distinct reflection bands within the plateau of the measured reflection spectra is coincidental. It shows that, depending on the specimen or the analyzed area, the layers are more or less organized by batches of similar thickness. The gold aspect arising due to high broadband reflectance in the visible range (blue region excluded) only requires the layer thicknesses to be in or around the appropriate mean value and to vary substantially across depth, without the need of a particular order or grouping in layer thickness values. This was also confirmed in the simulations. The high broadband reflectance was obtained irrespective of the fact that layer thickness decreases with

Fig. 1. A–C. Color pattern and elytral structure. **A**. *Charidotella ambita* habitus (sog: semi-ovoid gold patch; lgr: lateral gold ring; em: explanate margin). Lines D and I designate the location and orientation of the semi-thin sections in the elytra (**D**) and pronotum (**I**). **B**. SEM view of the ventral surface of the elytron, taken at an orientation that best visualizes the various elements of the locking device. The frame locates the locking device that is enlarged in **C**. (fl: flange; lc: longitudinal carina; mr: marginal ridge). **D–I**. Light microscopy (tb: trabecula; ML: multilayer). **D**. Transverse section of the elytron along line D in **A**. From left to right, successive black and gold regions of the disc followed by the transparent explanate margin. The frames indicate parts that are enlarged in Figures **E**, **F**, **H**. Note occurrence of pigment at cuticle periphery in the black regions (**F** and right half of **G**). Transition between pigmented and non-pigmented regions is indicated with black arrowheads. **G**. Junction between the semi-ovoid gold region (left) and the black region (right); the black arrow indicates the border of the pigment in the black region, the white arrow the border of the multilayer in the gold region **I**. Longitudinal section of the pronotum along line I in **A**. From left to right, the transparent explanate margin, the marginal gold ring and the black disc. The framed area is enlarged in the inset.

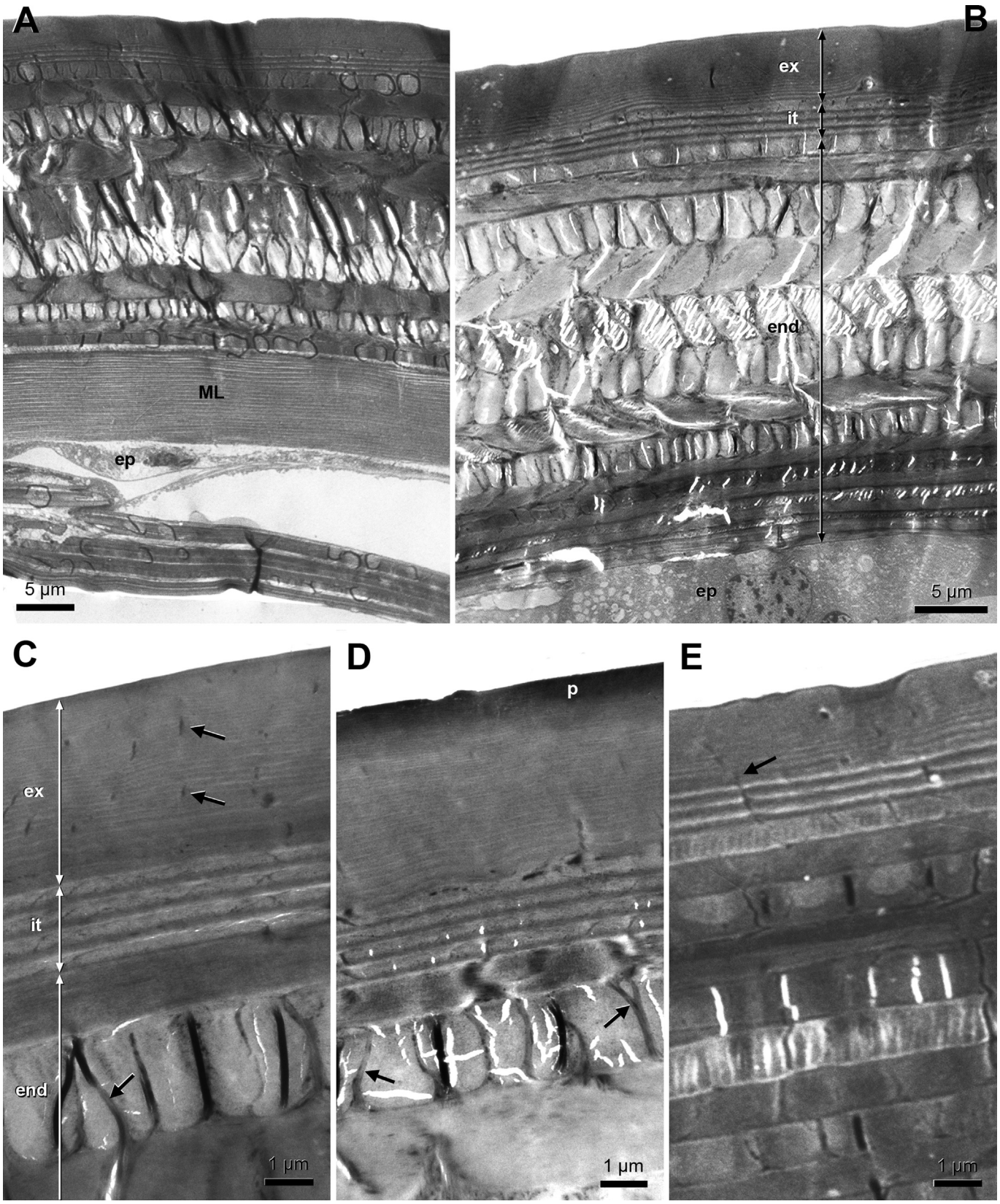

Fig. 2. Ultrastructure of the elytron. ex: exocuticle; end: macrolayer endocuticle; ep: epidermis; it; intervening transition between the exo- and endocuticles; ML: multilayer; p: pigment. **A**. Cross section in the elytron of the semi-ovoid gold region. The multilayer is located between the endocuticle and the epidermis. **B**. Cross section of the dorsal cuticle in the black region. **C**., **D**., **E**. Upper part of the dorsal cuticle in, respectively, the semi-ovoid gold region, the black region with surface pigment, and the explanate margin. Arrows indicate pore canals.

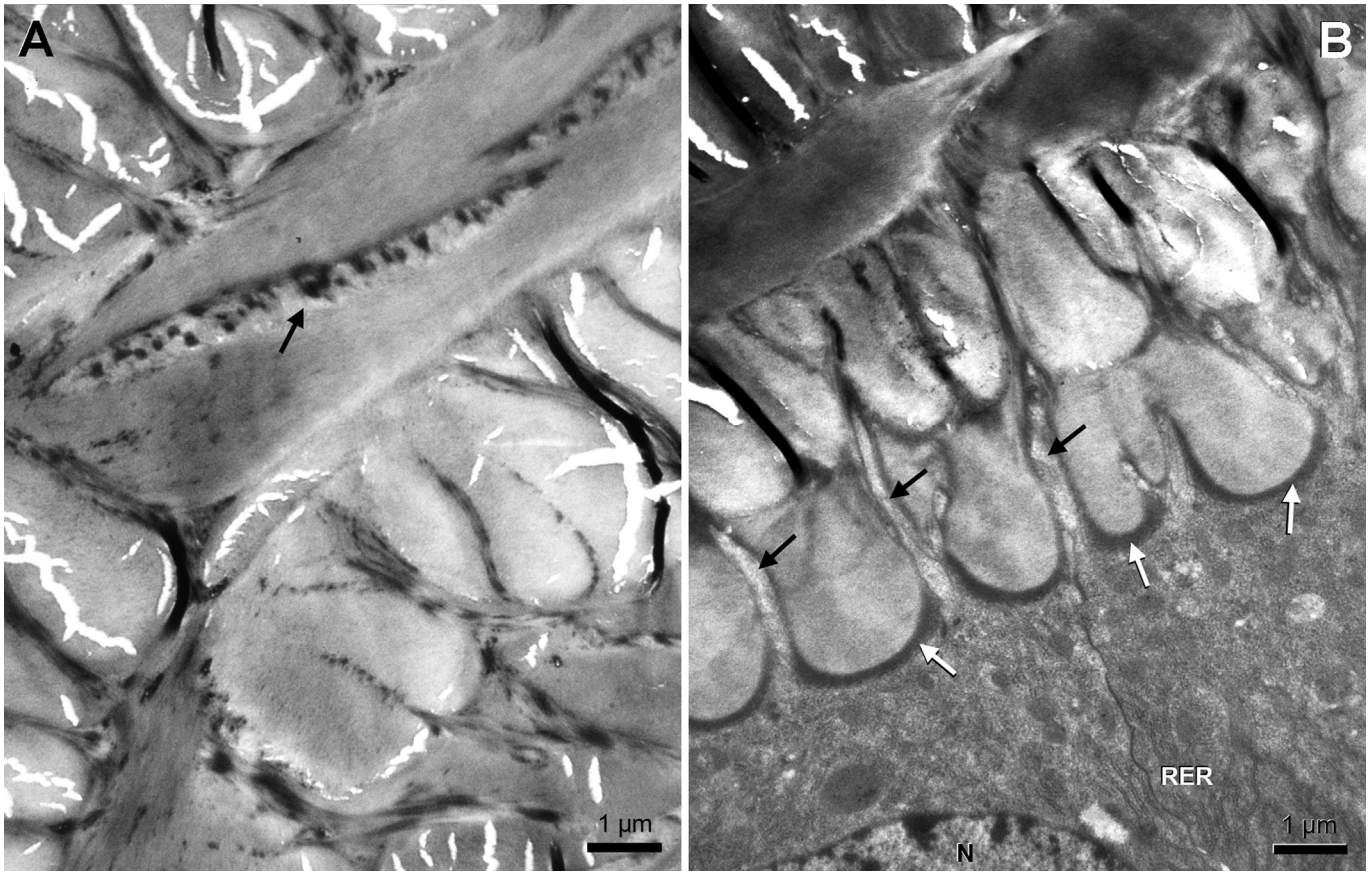

Fig. 3. A. Macrofiber endocuticle of a mature adult. Note the sinuous road of the pore-canal network with electron-dense fibers (arrow). **B**. Macrofiber endocuticle and pore-canal network secreted by the epidermis in a young adult. N: nucleus; RER: granular endoplasmic reticulum. The black arrows indicate formation of pore canals by cytoplasmic expansions, the white arrows indicate deposition of chitin microfibrils by plasma membrane plaques.

depth. Where layer thickness does decrease (Fig. 5), we obtain an intuitive way to understand the broadband reflectance: longer wavelengths are first reflected as light propagates inside the endocuticle and interferes locally with layers of larger thickness. However, even a random arrangement of thicknesses is able to produce such a high broadband reflectance, as is known, for instance, in the "chaotic" type of the chirped reflector of silvery fish skin (McKenzie et al., 1995). In the *C. ambita* chirped reflector, the number of bilayers determines the broadness of the high reflection plateau, the MLSO1-2 exhibiting a broader simulated spectrum than the areas with fewer bilayers MLSO3 and MLER where the multilayer tends to fuse to the cuticle.

The gold reflector is a local specialization of the endocuticle formed during the final stage of endocuticle macrofiber synthesis in young adults. Whereas in non-reflecting regions where few macrofibers are deposited, the epidermis shifts to the formation of the reflector in gold regions. To fully demonstrate this, the formation of the endocuticle following adult eclosion needs to be studied in greater detail. This was not possible with *C. ambita*, but preliminary observations on two other cassids with gold reflecting designs, *Charidotella propinqua* and *Chelymorpha alternans*, substantiated this view (Pasteels and Billen, unpublished). The progressive fusion of dark layers with the endocuticle macrofibers observed when both structures are in contact demonstrates that the dark layers of the reflector are made up of chitin in a protein matrix. The periphery of dark layers is more electron-dense than their center, suggesting that chitin micofibrils are more densely packed when in contact with the pale layers. Microfibrils are observed at the surface of the dark layers and in its center. Pale layers contain few microfibers seemingly arising from the surface of the dark layers. Improved description of the layers will require observation at higher resolutions.

The location of the gold reflector at the bottom of the endocuticle and its chirped structure agree with Hinton's (1973) pioneering description of the *Aspidiomorpha tecta* gold reflector (see also Parker et al., 1998). Preliminary observations (Pasteels and Billen) show that endocuticular reflectors are widespread in tortoise beetles, observed so far in five other species from three genera in three tribes including both species that are able and unable to reversibly change color (*Charidotella egregia*, *Ch. propinqua*, *Ch. sexpunctata*, *Chelymorpha alternans*, and *Coptocycla stigma*). A multilayer in the endocuticle sitting just above the epidermis is present in *C. egregia*, although previous study of dry elytra (Vigneron et al., 2007b) failed to detect it in this species. The location of the reflector just above the epidermis and the connection between its largely liquid pale layers by gaps in the dark layers facilitate the evolution of reversible color changes by injecting or resorbing liquid in the pale layers (Hinton, 1973; Vigneron et al., 2007b). Whether the reversible reflectors in Neotropical *Charidotella* species (Cassidini) and Paleotropical Aspidimorphini are independently evolved features remains to be investigated.

To the best of our knowledge an endocuticular metallic reflector is unique to the tortoise beetles among adult insects. However, an impressive endocuticular metallic reflector was described in Danainae (Lepidoptera, Nymphalidae) pupae (Steinbrecht, 1985; Steinbrecht et al., 1985). This reflector, called METAL for Multiple

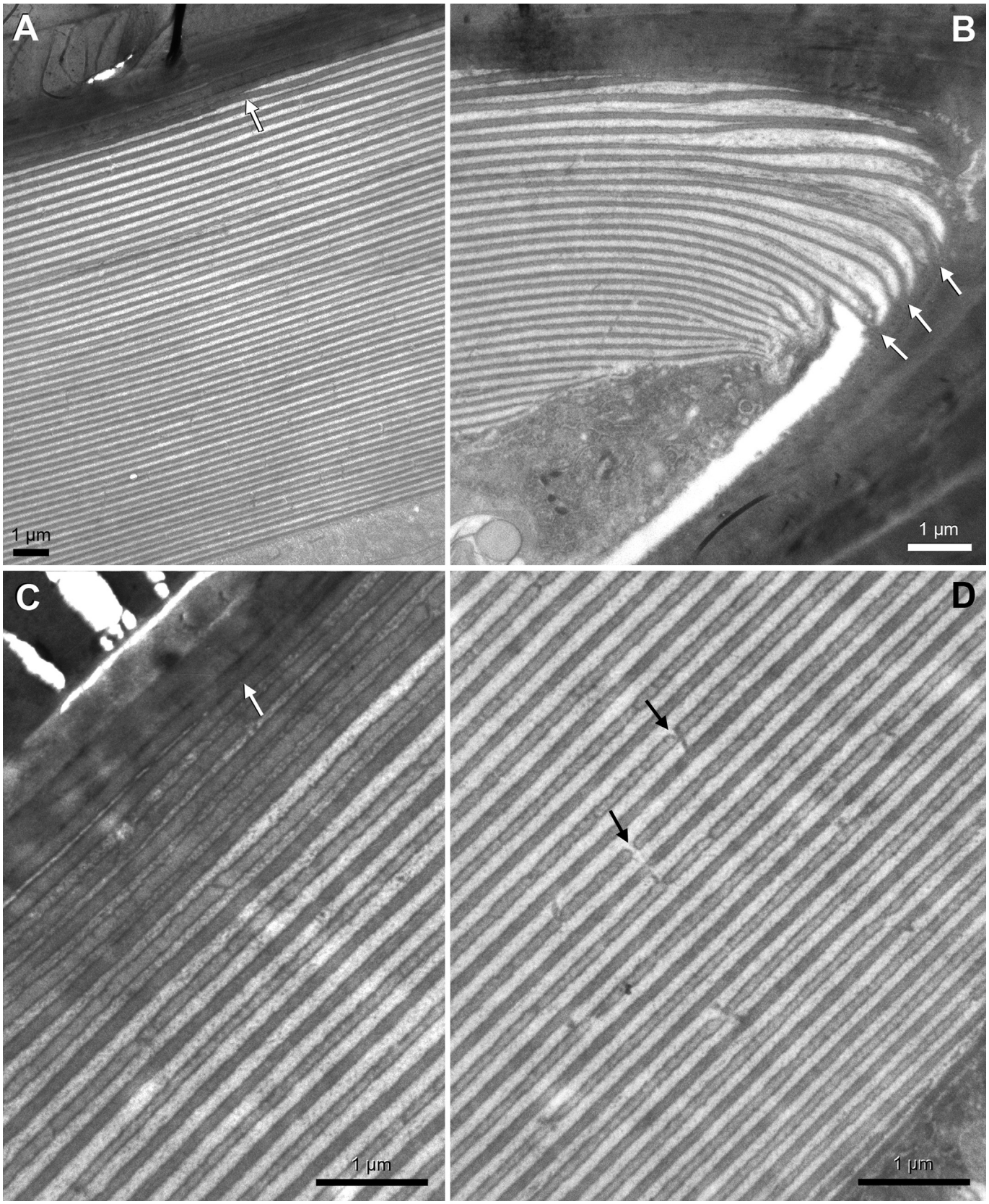

Fig. 4. Ultrastructure of the endocuticular multilayer of the semi-ovoid gold region. **A**. MLSO1. **B**. MLSO3. **C**. and **D**. Top and bottom of MLSO1. Note the regular and chirped structure of the multilayer; the fusion of dark layers (white arrows) with the endocuticle on top (**A**, **B**, **C**) or with a trabecula (**B**); the microfibrils at the surface of the dark layers reaching the pale layers (**C**, **D**) and gaps (black arrows) in the dark layers (**D**).

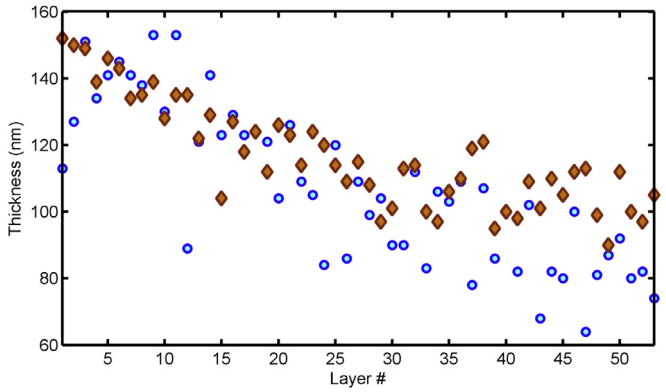

Fig. 5. Thicknesses of alternating pale (circles) and dark layers (diamonds) of MLSO1.

Endocuticular Alternating Layers, shows striking structural and functional similarities with that of *C. ambita*. It is made of up to 270 bilayers of dense (cuticular) and clear (aqueous) layers showing a highly regular organization with a systematic increase and decrease in clear layer thickness. As in tortoise beetles, the clear layers and gold color vanish in dried cuticle, but are partly restored by immediate re-wetting. In contrast to the *C. ambita* reflector, however, it composes the bulk of the endocuticle, being only dorsally limited by few dense layers of normal endocuticle and above the epidermis by 20–50 dense layers without any clear layers (Steinbrecht, 1985).

Thus far, structural colors in beetles are reported to result from various structures, i.e. diffraction gratings, multilayers or three-dimensional photonic crystals, all located in upper strata of the cuticle, epicuticle, exocuticle, or scales in curculionids and cerambycids (review in Seago et al., 2009). These first cuticular strata, contrary to the endocuticle, are largely formed in the pupa and present at hatching. Hence structural colors are present very early, at most only a few hours after the full sclerotization of the exocuticle. The deep endocuticular location of the multilayer reflector in *C. ambita* and likely other Cassidini raises intriguing questions on the *raison d'être* of gold color in tortoise beetles, as the reflector needs days or even weeks to develop. Barrow (1979) reported that metallic color took 14–27 days to appear in *Metronia bicolor* (synonym of *Charidotella sexpunctata*) and 9–18 days in *Deloyala guttata*. In *C. alternans* it took 13–17 days (Pasteels, unpublished observation). By contrast in the Danainae pupae, the METAL reflector develops shortly after pupal ecdysis. Synthesis of its bilayers starts 20 h after pupal ecdysis, and gold reflection appears after around 30 h, although bilayer formation continues until 48 h after ecdysis (Steinbrecht, 1985).

The function of metallic colors in beetles has been the topic of much speculation (review in Seago et al., 2009). In many leaf beetles bright colors linked to chemical defense act as aposematic

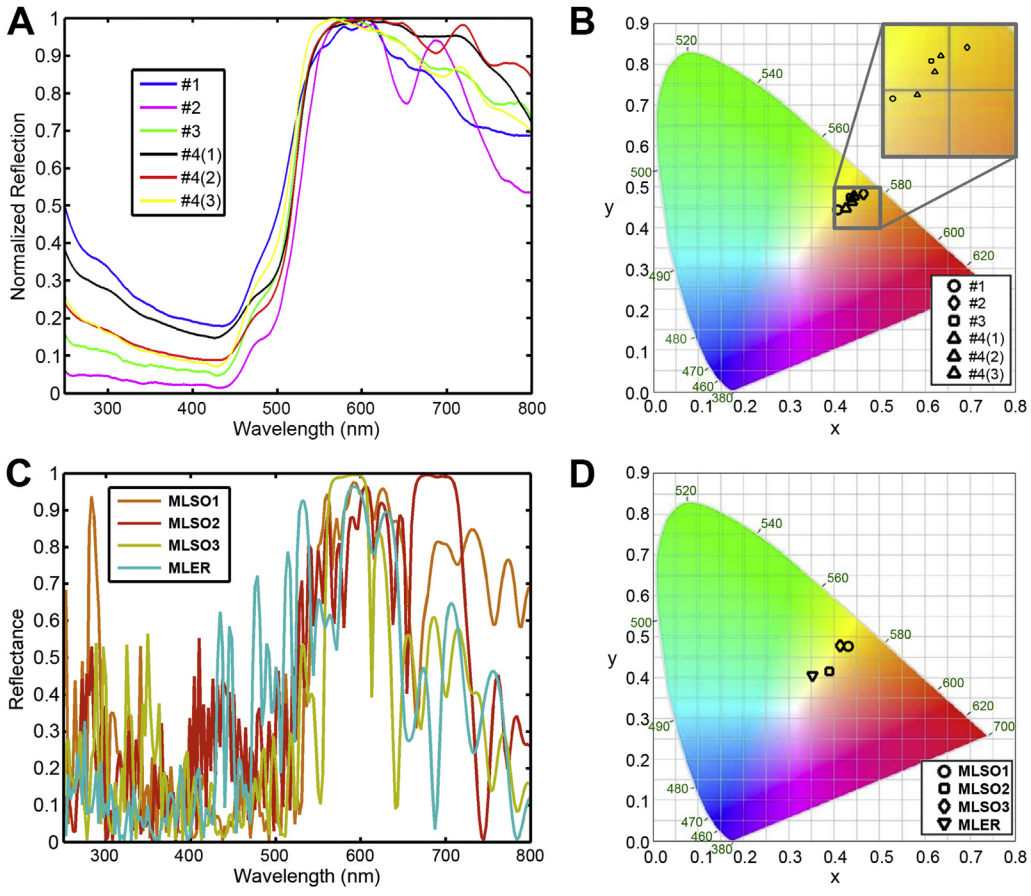

Fig. 6. A. Reflection spectra measured at normal incidence on the elytron semi-ovoid gold patch on freshly dead (#1) and live specimens (#2, #3, #4). Spectral variations exist among specimens and between successive measurements on the same live specimen, #4 (1, 2, 3). In the former case, variations are due to inherent variability in the multilayer from one specimen to another. In the latter case, variations are due to unavoidable fluctuation of the light spot position on the sample. **B**. Chromaticity coordinates calculated from measured reflection spectra in **A**. All points are located in the yellow region of the CIE diagram. **C**. Simulated reflectance spectra for multilayers in the semi-ovoid patch and lateral ring of the elytron. **D**. Chromaticity coordinates calculated from simulated reflectance spectra in **C**. All points are located in the yellow region showing good agreement with the measurements (**B**).

signals learned by predators. This is the case for the metallic *Chrysolina* leaf beetles secreting cardenolides when attacked (Pasteels and Daloze, 1977; Pasteels et al., 1979). The *Chrysolina* reflector, however, is located in the exocuticle (Vigneron et al., 2007a) and full color appears at hatching or within a few hours before the beetles reach their food plant from the ground in which they pupated. Evidence of chemical defense in adult tortoise beetles is thus far lacking. Alternatively, the golden appearance of tortoise beetles has been suggested to mimic rain drops under sunshine or to act as a mirror reinforcing homochromy (Hinton, 1973; Jolivet, 1994). Changing colors are possibly a mechanism that confuses predators. The strong contrast of colors between gold and adjacent black regions enhances visual appearance and argues for a signaling function. Without entirely rejecting a defensive function for gold reflection in tortoise beetles, a defense requiring a structure that takes days to develop in vulnerable young adults does not seem an optimal strategy. We speculate that a putative defensive function could be secondary but not likely the primary source of selection for gold reflection. Instead, we suggest that gold color may have evolved as an intraspecific, sexual, signal, even without sexual dimorphism. In *C. alternans*, after approximately two weeks of development, gold designs appeared suddenly in a mere two or three days. First copulations were observed in the same beetles only after full development of the gold reflector, but never before. Barrow (1979) reported that copulation occurred in *M. bicolor* (= *Ch. sexpunctata*) when they were from 14 to 17 days old, i.e. when the gold reflector was fully functional. Gold patterns could signal sexual maturity to conspecific partners. Admittedly this adds more speculation to the discussion, but is not necessarily lacking value, if it stimulates further behavioral and ecological investigations of tortoise beetles and their starling colors, defenses and reproductive habits.

Acknowledgements

We are very grateful to An Vandoren for her help in section preparation, and to R.A. Steinbrecht and two anonymous reviewers for valuable comments on the manuscript. SRM was supported by the Belgian National Fund for Scientific Research (F.R.S.-FNRS) as a Research Fellow and by Wallonia-Brussels International (WBI) through a Postdoctoral Fellowship for Excellence program WBI.WORLD. JMP and DMW received important logistical support from STRI during field work in Panama.

Dedication

We dedicate this paper to the memory of our colleague and friend Jean-Pol Vigneron whose enthusiastic interest in Panamanian metallic tortoise beetles was at the origin of this study.

Appendix A. Supplementary data

Supplementary data related to this article can be found at http://dx.doi.org/10.1016/j.asd.2016.10.008.

References

Barrow, E.M., 1979. Life cycles, mating, and color change in tortoise beetles (Coleoptera: Chrysomelidae: Cassidinae). Coleopt. Bull. 33, 9–16.
Berthier, S., 2007. Iridescences. The Physical Colors of Insects. Springer-Verlag, New-York.
Chamberlin, G.J., Chamberlin, D.G., 1980. Colour: its Measurement, Computation and Application. Heyden & Son Ltd, London.
Crowson, R.A., 1981. The Biology of the Coleoptera. Academic Press, London.
Hinton, H.E., 1973. Some recent work on the colours of insects and their likely significance. Proc. Brit Ent Nat. Hist. Soc. 6, 43–54.
Imms, A.D., 1934. A General Textbook of Entomology. Methuen & Co, London.
Ingram, A.L., Deparis, O., Boulenguez, J., Kennaway, G., Berthier, S., Parker, A.R., 2011. Structural origin of the green iridescence on the chelicerae of the red-backed jumping spider, *Phidippus johnsoni* (Salticidae: Araneae). Arthropod Struct. Dev. 40, 21–25.
Jolivet, P., 1994. Physiological colour changes in tortoise beetles. In: Jolivet, P., Cox, M.L., Petitpierre, E. (Eds.), Novel Aspects of the Biology of Chrysomelidae. Kluwer Academic Publ., Dordrecht, pp. 331–335.
Judd, D.B., Wyszecki, G., 1975. Color in Business, Science and Industry. John Wiley & Sons, New York.
Leertouwer, H.L., Wilts, B.D., Stavenga, D.G., 2011. Refractive index and dispersion of butterfly chitin and bird keratin measured by polarizing interference microscopy. Opt. Express 19, 24061.
Leopold, R.A., Newman, S.M., Helgeson, G., 1992. A comparison of cuticle deposition during the pre- and posteclosion stages of the adult weevil, *Anthonomus grandis* Boheman (Coleoptera: Curculionidae). Int. J. Insect Morphol. Embryol. 21, 37–62.
Mason, C.W., 1929. Transient color changes in the tortoise beetles (Coleop.: Chrysomelidae). Entomol. News 40, 52–56.
McKenzie, D.R., Yin, Y., McFall, W.D., 1995. Silvery fish skin as an example of a chaotic reflector. Proc. R. Soc. A 451, 579–584.
McPhedran, R.C., Parker, A.R., 2015. Biomimetics: lessons on optics from nature's school. Phys. Today 68, 32–37.
Neville, A.C., 1977. Metallic gold and silver colours in some insect cuticle. J. Insect Physiol. 23, 1267–1274.
Neville, A.C., Caveney, S., 1969. Scarabaeid beetle exocuticle as an optical analogue of cholesteric liquid crystals. Biol. Rev. 44, 531–562.
Parker, A.R., Mc Kenzie, D.R., Large, M.C.J., 1998. Multilayer reflectors in animals using green and gold beetles as contrasting examples. J. Exp. Biol. 201, 1307–1313.
Pasteels, J.M., Daloze, D., 1977. Cardiac glycosides in the defensive secretion of Chrysomelid beetles. Science 197, 70–72.
Pasteels, J.M., Daloze, D., Van Dorsser, W., Roba, J., 1979. Cardiac glycosides in the defensive secretion of *Chrysolina herbacea* (Coleoptera, Chrysomelidae). Identification, biological role and pharmacological activity. Comp. Biochem. Physiol. 63, 117–121.
Schneider, C.A., Rasband, W.S., Eliceiri, K.W., 2012. NIH Image to ImageJ: 25 years of image analysis. Nat. Methods 9, 671–675.
Seago, A.E., Brady, P., Vigneron, J.-P., Schulz, T.D., 2009. Gold bugs and beyond: a review of iridescence and structural colour mechanisms in beetles (Coleoptera). J. R. Soc. Interface 6, S165–S184.
Sollas, I.B.J., 1907. On the identification of chitin by its physical constants. Proc. R. Soc. Lond B 79, 474–481.
Stavenga, D.G., Wilts, B.D., Leertouwer, H.L., Hariyama, T., 2011. Polarized iridescence of the multilayered elytra of the Japanese jewel beetle, *Chrysochroa fulgidissima*. Phil Trans. R. Soc. B 366, 709–723.
Steinbrecht, R.A., 1985. Fine structure and development of the silver and golden cuticle in butterfly pupae. Tissue Cell 17, 745–762.
Steinbrecht, R.A., Mohren, W., Pulker, H.K., Schneider, D., 1985. Cuticular interference reflectors in the golden pupae of danaine butterflies. Proc. R. Soc. Lond B 226, 367–390.
van de Kamp, T., Riedel, A., Greven, H., 2016. Micromorphology of the elytral cuticle of beetles, with an emphasis on weevils (Coleoptera: Chrysomelidae). Arthropod Struct. Dev. 45, 14–22.
Vigneron, J.-P., Lousse, V., 2006. Variation of a photonic crystal color with the Miller indices of the exposed surface. Proc. SPIE 6128, 61281G.
Vigneron, J.-P., Rassart, M., Vandenbem, C., Lousse, V., Deparis, O., Biró, L.P., Dedouaire, D., Cornet, A., Defrance, P., 2006. Spectral filtering of visible light by the cuticle of metallic wood boring beetles and microfabrication of a matching bioinspired material. Phys. Rev. E 73, 041905.
Vigneron, J.P., Colomer, J.-F., Rassart, M., Lousse, V., Naji, S., Ertz, D., 2007a. Structural coloration of a native iridescent leaf beetle: *Chrysolina fastuosa*. Phys. Mag. 28, 239–248.
Vigneron, J.-P., Pasteels, J.M., Windsor, D.M., Vértesy, Z., Rassart, M., Seldrum, T., Dumont, J., Deparis, O., Lousse, V., Biró, L.P., Ertz, D., Welch, V., 2007b. Switchable reflector in the Panamanian tortoise beetle *Charidotella egregia* (Chrysomelidae: Cassidinae). Phys. Rev. E 76, 031907.